Pergamon

Geochimica et Cosmochimica Acta, Vol. 67, No. 23, pp. 4519–4527, 2003

0016-7037/03 $30.00 + .00

doi:10.1016/S0016-7037(03)00410-1

Strontium in coral aragonite: 2. Sr coordination and the long-term stability of coral environmental records

ADRIAN A. FINCH[1,2,*] and NICOLA ALLISON[2]

[1]Centre for Advanced Materials, University of St Andrews, St Andrews, Fife KY16 9AL, UK
[2]School of Geography & Geosciences, University of St Andrews, Irvine Building, St Andrews, Fife KY16 9AL, UK

(*Received January* 7, 2003; *accepted in revised form May* 20, 2003)

Abstract—We have used X-ray Diffraction (XRD) and Sr K-edge Extended X-ray Absorption Fine Structure (EXAFS) to determine the structural state of Sr in a suite of coral aragonite samples. Our samples encompassed a selection of coral species (*Porites lobata*, *Porites lutea*, *Pocillopora eydouxi*, *Montastrea annularis*, *Pavona gigantea* and *Pavona clavus*) including some commonly used for palaeoenvironmental reconstruction. Aragonite was the only carbonate observed by XRD. We refined the isolated EXAFS against structural models for Sr in aragonite and two-phase strontianite/aragonite mixes. Our data are indistinguishable from Sr ideally substituted in aragonite and strontianite was present below detection levels (estimated at $<5\%$ of Sr present). Comparisons of recent and ancient coral aragonite show no sign of exsolution, either by spinodal decomposition or by the direct nucleation of strontianite domains. Published diffusion rates of Sr in ionic solids support the view that exsolution would occur prohibitively slowly. Coral aragonites are metastable materials with slow diffusion kinetics that have the potential to encode environments over timescales of millions of years. *Copyright © 2003 Elsevier Ltd*

1. INTRODUCTION

Tropical coral skeletons indicate great promise as proxies of past sea surface temperatures (SSTs) as the geochemistry of the skeleton may encode the environment at the time of skeletal deposition. SSTs have been inferred from the Sr/Ca ratios of coral aragonite (e.g., de Villiers et al., 1994) and analysis of fossil corals has been used to estimate past SSTs (e.g., McCulloch et al., 1999). However there are considerable variations between the palaeothermometers reported by authors working at different sites (e.g., Beck et al., 1992; Beck, 1994; de Villiers et al., 1994, Alibert and McCulloch, 1997) and even variations in the palaeothermometers calculated from different individual corals at the same site (de Villiers et al., 1995). Because of this estimates of SST from the same Sr/Ca ratio can differ by up to 3–4°C depending on the palaeothermometer relationship used.

The reason for these variations is unclear. The Sr/Ca ratio of coral aragonite may be affected by e.g., calcification rate (de Villiers et al., 1995) or thermal stress (Marshall and McCulloch, 2002). However an outstanding issue with regard to the use of the Sr palaeothermometer is the mode of incorporation of Sr in coral carbonate. Sr concentrations in corals are high (usually 7500 ± 500 ppm) and exceed the thermodynamic solubility level of Sr ideally substituted in aragonite (Plummer and Busenberg, 1987). It has been suggested that some coral skeletons may contain Sr distributed between two phases: as Sr ideally substituted for Ca in aragonite and as discreet $SrCO_3$ (strontianite) domains (Greegor et al., 1997). The structural state of Sr in coral aragonite has implications for the Sr palaeothermometer relationship since the free energy of formation of a solid solution is different from that of a two-phase mixture, and therefore trace element partitioning will be significantly dependent on Sr structural state. The relative proportion of Sr in strontianite and aragonite coordinations may vary between individuals of the same species (Greegor et al., 1997) and could therefore explain why some individuals exhibit different Sr/Ca palaeothermometer relationships.

The present paper examines the structural state of Sr in a variety of coral species. First, we determine the dominant minerals present in the skeletons using X-ray Diffraction (XRD) and then use Extended X-ray Absorption Fine Structure (EXAFS) to determine the Sr coordination in the coral skeletons. We determine the relative proportions of Sr in the strontianite and aragonite coordination in corals of different taxa, provenances and age, and we also examine multiple individuals of the same species including material precipitated at different rates. We relate the Sr structural state to these parameters to determine whether Sr structural state varies in a predictable way and therefore whether criteria can be established that would allow more reliable palaeoenvironmental reconstructions. For example, individual coral skeletons that contain little or no strontianite may prove to be more reliable as palaeoenvironmental indicators.

2. SAMPLES

Details of the samples analyzed in the present study are summarised in Table 1. This table includes information on the collection sites, including annual seawater temperature ranges, and refers to previously published work using the coral material. The details of the corals collected from Oahu have not been previously published. These corals were collected in July/August 2000 and were soaked for ~3 h in sodium chlorate(I) (hypochlorite) to remove the coral tissue. The *Pocillopora eydouxi* specimens were collected from Kaneohe Bay in a water depth of ~ 10 m, and the *Porites lobata* were collected from Lanakai, in a water depth of ~ 2 m. The table also summarises the dates when the corals were collected and the approximate ages of the material analyzed. Unless stated oth-

* Author to whom correspondence should be addressed (aaf1@st-and.ac.uk).

Table 1. Details of sample sites, including the dates when the coral skeletons were collected, and the period when the studied material was deposited. The SST range corresponding to the depositional date is also given where known. Recent references on each skeleton are included where applicable.

Sample site (and reference)	Annual SST range (°C)	Coral species	Collection date	Deposition date of material studied	Sample Names
Ko Phuket, Thailand (1)	25–30	*Porites lutea*	1991	1989–1991	PB3, PB3_outer, PB3_untreat, PB4, PB4_outer, PB5_outer, PB6, PB6_outer
Oahu, Hawaii (2)	22–28	*Porites lobata*	2000	1997–2000	NA33_less_dense, NA35_less_dense, NA35_dense
	22–28	*Pocillopora eydouxi*	2000	1997–2000	Pocil_whole, Pocil_disep
Tarawa Atoll, W. Pacific (3,4)	27–29	*Porites lobata*	1990	1985–1990	Tarawa_modern
	unknown	*Porites lobata*	1990	1938–40	Tarawa_old
San Cristobal, Galapagos (5)	20–25	*Pavona clavus*	1992	1990–1992	Pavona_slide
Shirigai Bay, Japan (6)	16–29	*Porites lobata*	1993	1978–1993	Japan
Huon Peninsula, Papua New Guinea (PNG) (7,8)	27–30	*Porites*	1995	1978–1995	PNG_modern
	unknown	*Porites*	1995	130 ± 2 kyr BP	PNG_fossil
Champion Island, Galapagos	unknown	*Pavona gigantea*	unknown	unknown	PGC3
Puerto Rico	unknown	*Montastrea annularis*	unknown	unknown	2T3

From: Allison et al., 1996 (1), Allison and Finch, 2002 (2), Shen et al., 1992 (3), Cole et al., 1993 (4), de Villiers et al., 1994 (5), Fallon et al., 1999 (6), McCulloch et al., 1999 (7) and Tudhope et al., 2001 (8).

erwise, we analyzed material close to the coral surface but below the tissue layer. The amount of material analyzed usually corresponded to ~1–2 yr growth. We analyzed 6 different coral species representing a cross-section of the major species used for palaeoenvironmental reconstruction. We also arranged the samples into groups to compare the Sr coordination of corals in different sample suites, detailed in Table 2.

2.1. Sample Pretreatment

To investigate the effect of sample pretreatment on Sr, we analyzed aliquots of coral PB3 before and after sodium chlorate(I) (hypochlorite) treatment. Treated aliquots of this coral were soaked in a 3–4% solution of sodium chlorate(I) for 48 h and then rinsed in distilled water for 48 h. Note that in the present paper we use the term 'bleaching' to refer to the process

Table 2. Samples arranged into suites for comparison. Sample names are given in Table 1 - the full refinements of all samples are found in the electronic supplement.

Sample suite	Location	Sample name
Skeleton age (in *Porites spp.*)		
130 ka	PNG	PNG_fossil
50 yr	Tarawa Atoll	Tarawa_old
<10 yr	Japan and PNG	Japan, PNG_modern
<5 yr	All other samples	All other samples
Effect of sodium chlorate (I) treatment (in *P. lutea*)		
Treated samples	Thailand	PB3, PB4, PB6
Untreated sample	Thailand	PB3_untreat
Effect of coral bleaching (in *P. lutea*)		
Unbleached specimens	Thailand	PB3_outer, PB6_outer
Bleached specimens	Thailand	PB4_outer, PB5_outer
Effect of skeletal growth rate (in *P. lutea*)		
Slow growth (8 mm yr^{-1})	Thailand	PB4
Slow growth (12 mm yr^{-1})	Thailand	PB6
Fast growth (22 mm yr^{-1})	Thailand	PB3
Effect of density banding (in *P. lobata*)		
Dense bands	Hawaii	NA35_dense
Less dense bands	Hawaii	NA33_less_dense, NA35_less_dense
Skeletal macrostructure (in *Pocillopora*)		
Pocillopora whole sample	Hawaii	Pocil_whole
Pocillopora dissepiments	Hawaii	Pocil_disep

whereby symbiotic zooxanthallae are lost from the living coral, whereas the soaking of the sample before analysis is referred to as 'sample pretreatment'.

2.2. Skeletal Growth Rate

To investigate the effect of variations in skeletal extension rate on Sr incorporation, we compared three of the *Porites lutea* corals collected from Phuket, Thailand. These corals were sectioned along the axis of maximum growth and photographed under UV radiation to show fluorescent banding. Bright-dull fluorescent couplets represent approximately annual growth in these corals with bright band deposition beginning around November. We cut the same annual increment, representing material deposited approximately from November 1989 to November 1990, from each coral and measured the annual linear extension over this period. Skeletal extension for colonies PB4, PB6 and PB3 were 8, 12 and 22 mm respectively. Each sample was ground to a fine powder and subsampled for analysis.

2.3. Density Banding

To compare the Sr coordination of dense and less dense bands in the coral skeletons we cut small sample blocks from dense and less dense bands, visible by autoradiography, deposited in 1997–1998 from two *Porites lobata* colonies collected from Oahu. Again samples were ground to fine powders and subsampled for analysis.

2.4. Coral Bleaching

The coral skeletons from Phuket were collected in July 1991, during a coral bleaching event giving us the opportunity to investigate the effect of coral bleaching on skeletal Sr coordination. Bleached corals can precipitate aragonite which contains anomalously high Sr/Ca ratios (Marshall and McCulloch, 2002; N. Allison, unpublished data). This may be because thermal stress can affect the transport of Ca^{2+} and Sr^{2+} through the coral tissue causing an increase in the Sr/Ca ratio of the calcifying fluid (Marshall and McCulloch, 2002). Alternatively the decrease in skeletal calcification rate, associated with bleaching, may serve to increase the experimentally determined Sr/Ca partition coefficient (Rimstidt et al., 1998).

There were marked differences in the degree of bleaching between colonies at Phuket during 1991, with some colonies apparently unaffected (e.g., PB3 and PB6) while others appeared almost white (PB4 and PB5). Alizarin red S staining indicated that all of these colonies were still calcifying despite the high degree of bleaching in some individuals. We collected the outermost layer of skeletal material ($<$1 mm thick) from each colony by scraping the skeleton with a scalpel blade. This material was ground to a fine powder and subsampled for analysis.

2.5. Skeletal Architecture

Coral calcification is complex and results in the deposition of a range of skeletal structures. In particular, calcification occurs throughout the depth of the tissue layer and results predominantly in the deposition of vertical skeletal rod-like structures (Barnes and Lough, 1993). However the tissue layer is periodically uplifted and a horizontal layer or dissepiment is deposited, sealing the new tissue layer off from the remainder of the skeleton. The analysis of individual components of the skeletal architecture requires a precise microsampling that is practically very difficult. However, for coral species with relatively large calices it is possible to handpick some skeletal components and analyze them in isolation. We compared the Sr coordination of the skeletal dissepiments from a *Pocillopora eydouxi* with Sr coordination in the remainder of the skeleton. Dissepiments were handpicked using forceps from a slice of a *Pocillopora* skeleton, ground to a fine powder and subsampled for analysis.

3. ANALYTICAL METHODS

3.1. X-ray Diffraction (XRD)

All samples were ground to submicron powders in an agate mortar and pestle and then analyzed using XRD on an automated Philips PW1050 X-ray diffractometer. The primary X-ray beam was Co Kα radiation and the secondary X-rays were detected by scanning between 5 to 70° 2θ with a scan speed of 0.02° s^{-1}. The diffractometer was controlled using Philips WinXRD V2 software. Samples for XRD were identical to the powders used for EXAFS below.

3.2. Extended X-ray Absorption Fine Structure (EXAFS)

Aragonite is an orthorhombic polymorph of calcium carbonate with a structure that can be approximated to rhombic symmetry. Each metal ion (Sr or Ca) in the structure is surrounded in turn by 9 oxygen atoms (first shell), then 6 carbon atoms (second shell) and 6 metals (third shell). When Sr is randomly substituted in the aragonite, the nearest metals (in the third shell) are all Ca, whereas in strontianite, in which all the Sr atoms are clustered together, the third shell comprises entirely Sr atoms. Between these end-members, partly ordered states are possible, in which the number of adjacent Sr atoms lies between 0 and 6, representing incomplete ordering on the metal sites. Sr structural state in coral aragonite can be determined using the method of Extended X-ray Absorption Fine Structure (EXAFS). This is an analytical method that examines the way in which X-rays (generated in a synchrotron) are absorbed by the material, and provides information on the coordination state of trace elements in materials. Initial qualitative Sr K-EXAFS study of coral aragonite by Greegor et al. (1997) suggested variation in the Sr coordination states between different coral samples. In a subsequent quantitative study involving refinement and modelling of data, Sr K-edge EXAFS was performed on strontianite, Sr in aragonite and mechanically mixed standards (Finch et al., 2003) indicating that each of these coordination states was readily resolvable using the method. The two coordination states were distinguished by quite different values of two refinable parameters, R_3 and PERCA1. R_3 represents the interatomic distance between the central Sr and its nearest metal, which in the aragonite coordination is $\sim$4.018$\pm$0.010 Å, and in strontianite is 4.167$\pm$0.010 Å (errors are shown as absolute values). The parameter PERCA1, dependent on the phase angle of the electron interaction with the third shell, is scaled to vary from 0.99$\pm$0.11% in aragonite to 0.00$\pm$0.11% in strontianite. This parameter varies such that 0 Sr atoms in the third shell corresponds to PERCA1$=$1, and 6 Sr is represented by PERCA1$=$0. Two-phase states (i.e., a mixture of strontianite and aragonite) or partly ordered structural states (i.e., single-phase materials in which Sr is not randomly distributed) would be observed as deviations of R_3 and PERCA1 from the values for the appropriate standard. From analysis of a mechanical mixture, Finch et al. (2003) estimated that the limit of detection of strontianite coordination within aragonite coordination was $\sim$5% strontianite. We use identical methods of data collection and bulk refinement as those given by Finch et al. (2003).

3.3. EXAFS Data Collection

All samples were analyzed on station 16.5 at the SRS Daresbury synchrotron facility, Warrington, UK. Samples were presented to the

beam in an Al plate with a letterbox slot cut through it. Approximately 1 g of powder was sealed within the slot using sticky tape in front and behind the powder. The holder was positioned with respect to the beam such that the X-rays passed through the slot and did not encounter the holder. Measurements were taken with an average beam current of 200 mA. Station 16.5 receives X-rays from a 6 T wiggler. The station employs a dynamically focusing double crystal Si 220 monochromator, which brings 8 mrad of the fan to a horizontal focus at the sample, (spot size <2 mm). This is used in conjunction with a vertically focusing premirror for collimation and harmonic rejection. EXAFS was performed on the Sr K-edge. Count times were increased at higher energies to ensure improved signal-to-noise at higher k in the resultant EXAFS. For strontianite, analysis was in transmission mode, whereas for all other samples, fluorescence data were collected. In fluorescence mode, the emitted X-rays were collected using a 30-channel Ge-solid state detector running at 200 kHz per channel using dedicated fast counting electronics. Each channel counted the X-rays from the Sr Kα fluorescence and the resultant signal was the sum of the 30 channels. Final spectra were formed from the summing of two or more scans. Each sample took typically 2.5 h of beamtime. See www.srs.dl.ac.uk/srs/ for further details of the beamlines and sample holders.

3.4. EXAFS Data Analysis

Data analysis was carried out on software made available by the Daresbury site. Backgrounds were removed from the data using SPLINE (Paul Ellis, University of Sydney, 1990), and phase-shifted Fourier transforms of the data to provide the radial distribution functions were carried out using EXCURV98 (Daresbury Laboratories, UK). Interatomic distances and thermal vibration factors were refined to minimize the squares of residuals between the unfiltered data and the model spectrum using single scattering on EXCURV98. Unless otherwise stated, refinements were carried out within a k-range of 2 to 11 and the R range is 1.6 to 4.5 Å. Under these conditions, the numbers of independent parameters supported by the data ($N = 2\Delta k\Delta R/\pi + 1$) are ~17.6, significantly greater than the numbers of variables in the fitting procedure ($P = 8$), giving a determinacy (N/P) of 2.2. The fit index (R) is defined as:

$$R = \sum_i \left[\frac{1}{\sigma_i} \left\{ \left| \text{experiment}_i - \text{theory}_i \right| \right\} \right] \times 100\%$$

where:

$$\frac{1}{\sigma_i} = \frac{k_i^3}{\sum_i [k_i]^3 \times |\text{experiment}_i|}$$

experiment_i is the value of χ_{exp} at the point i, and theory_i is χ_{theory} at point i. Errors relate to the displacements in each value required to cause a 2.5% increase in the optimum fit. During the data processing, note that the energy of the absorption edge is initially judged by eye and then refined more precisely as the parameter E_f. For that reason, there is no significance to the way that E_f varies between refinements, merely representing the vagaries of that initial judgement.

4. RESULTS

XRD analysis of all the corals detected aragonite as the only phase, but with occasional minor diffraction peaks corresponding to sodium chloride. These may have been introduced by the chlorate(I) pretreatment, or by the dehydration of trapped seawater. XRD is, however, insensitive to small (e.g., <3%) volumes of minor phases. If, for example, small amounts of other carbonates such as strontianite had been present, these would not have been detected by XRD.

All the raw EXAFS data and fits in the present study are available as an Electronic Annex (see Elsevier Website, Science Direct), but selected isolated EXAFS oscillations are presented in Figure 1. Initially, we modelled the raw data as single-phase aragonite, refining the edge energy (E_f), the interatomic distances (R_1, R_2, R_3), thermal vibration parameters σ^2_1, σ^2_2, σ^2_3 and the percentage of Ca in the third shell (PERCA1) (see Finch et al., 2003). The initial values were set to those of a Sr in aragonite standard (Finch et al., 2003) and allowed to refine by minimizing the fit indices. The parameters corresponding to the best fits are given in Table 3 and the model isolated EXAFS associated with the refinements are present as fine lines on Figure 1. Analysis of the standards under the same conditions gave fits with R-factors ~24% (Finch et al., 2003 and Table 3) and all the coral samples analyzed refine as single-phase material with comparable R-factors. In addition, all R_3 and PERCA1, sensitive to partly ordered states, refine with two exceptions (PB3 and Tarawa_modern) to values within error of the Sr in aragonite standard. The refinement of a third coral, PGC3, also refines to a low value (0.90 ± 0.11) but the error associated with this parameter meant that the value still overlaps with 1. Some refinements (e.g., Pavona_slide) give PERCA1 values greater than 1. Such values have no physical meaning since PERCA1=1 implies that the site is completely populated with Ca. However in every case, the value overlaps with 1 within error. In the two anomalous refinements where PERCA1 does not equal 1 within error, the optimum values (0.91 ± 0.05, Tarawa_modern) and (0.87 ± 0.11, PB3) might indicate a partly Sr ordered state with ~10% ordering. However, the refinements are relatively insensitive to variations in PERCA1, and moving these values to 0.96 and 0.98 merely causes a 2.5% increase in the fit index. These values are very close to the expected value of 0.99. Furthermore, for refinements of partly ordered states, we expect decreases in PERCA1 to be coupled with increases in R_3 as the refinements grade between the parameters of the Sr in aragonite and strontianite structural states. For example, for 10% Sr ordering, R_3 would increase by ~0.015 Å from 4.020 Å (in aragonite) to ~4.035 Å (10% ordered). This difference lies beyond the refinement error of 0.011 Å and would therefore be resolvable, i.e., R_3 is a more reliable indicator of partly ordered states. In the two samples discussed above, the refinements provide R_3 values within error of the Sr in aragonite standard. We therefore do not attribute any significance to these anomalous values of PERCA1 in the refinements.

We then refined the data as two-phase strontianite/Sr in aragonite mixtures. The parameters for each coordination state were taken from the optimum values from refinement of the standards (Finch et al., 2003), and we refined only the edge energy (E_f) and the % of each phase. Such analysis did not improve the quality of the fits (including the two anomalous refinements), and in every case, the optimum R-factors applying this model were achieved when the strontianite content was within error of 0%. These observations provide no evidence for the presence of significant strontianite in any of the corals studied above the estimated limit of detection (~5%, Finch et al., 2003). Therefore we infer that all of the corals studied, irrespective of locality, age, taxon, growth rate etc. have Sr ideally substituted in aragonite as the sole detectable coordination state.

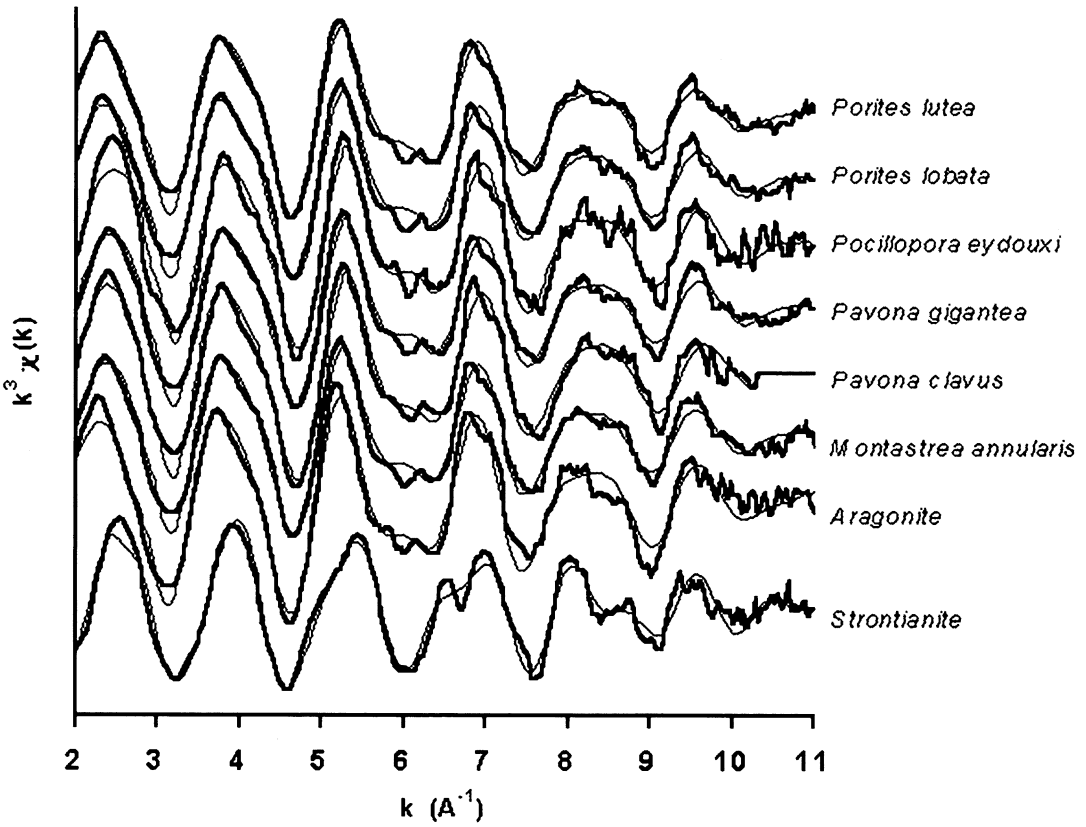

Fig. 1. Isolated EXAFS oscillations for the different coral species analyzed. The bold lines are the raw data, the fine lines are model EXAFS based on fits generated using the refinement parameters in Table 3. Two standard materials (aragonite and strontianite) are presented at the bottom. The samples illustrated are PB4 (*P. lutea*), Japan (*P. lobata*), Pocil_whole (*P. eydouxi*), PGC3 (*P. gigantea*), Pavona_slide (*P. clavus*) and 2T3 (*M. annularis*).

5. DISCUSSION

Our quantitative data showing that all the corals refine to single-phase aragonite is contrary to the qualitative observations of Greegor et al. (1997), but in accordance with the data of Allison et al. (2001) and Finch et al. (2003). Note that Finch et al. (2003) analyzed material previously used by Greegor et al. (1997) and interpreted by those authors as comprising dual-phase material. Finch et al. (2003) found no evidence for such behaviour. All corals studied precipitate a metastable, Sr-supersaturated aragonite with strontianite below detection levels (<5% of the total Sr). Analysis of the present data suggests that strontianite is not widespread in coral aragonite.

This observation has significant implications for the long-term stability of coral aragonite and therefore the palaeoclimatic records potentially encoded within them. Sr-supersaturated aragonite is not the lowest free energy state of that composition, and therefore may break down (exsolve), modifying its chemistry with time. Exsolution may occur by one of three mechanisms. The first, dissolution/reprecipitation, occurs when the aragonite is dissolved into aqueous solution and then replaced by precipitation of a secondary mineral. This secondary phase is likely to be calcite, the thermodynamic equilibrium phase of calcium carbonate. Such a process may be essentially instantaneous when considered against geological timeframes. We have analyzed all of the corals by XRD to determine whether calcite is present and we find no evidence for any carbonate phase other than aragonite. Furthermore, solution reprecipitation would be associated with significant textural change in thin section, which is not observed in thin sections of our samples. Some calcite overgrowths may occur in older samples, but calcite is relatively poor in Sr compared with aragonite, and so contributes little to the total Sr present. This suggests that significant modification of the chemistry of the skeletons by solution reprecipitation has not occurred in any of the samples.

The second mechanism for exsolution, spinodal decomposition, occurs by the formation of Sr-rich and Sr-poor domains in which the state of order progressively increases with time. This exsolution mechanism relies on the internal diffusion of ions, driven by the free energy contrast between the initial, transition and end states, ultimately giving rise to a two-phase strontianite/Sr in aragonite mix. The ultimate product of spinodal decomposition would be a mixture of the compositions at the solvus, but intermediate stages would involve the formation of partly ordered structural states, in which Sr had started to cluster into non-random distributions. This would be recognized in EXAFS data as single-phase refinements in which PERCA1 and R_3 values are midway between the two standards. In two refinements (Tarawa_modern and PB3_untreat), the maximum PERCA1 value lies below <0.99, but the R_3 of these

Table 3. Parameters of the optimum FINAL EXAFS refinements using a single-phase aragonite model. σ^2_1, σ^2_2 . . . refer to the thermal vibrational parameters (in Å^2) of each shell, and R_1, R_2 . . . refer to the interatomic bond distances of the same shells (Å). Errors in the last digit are in parentheses, calculated as the average offsets from the optimum values that cause a 2.5% increase in the Fit Index. (F) implies that the Parameter is fixed for the refinements.

Genus Sample name	Aragonite T7	Strontianite Stront	*Montastrea annularis* 2T3	*Pavona clavus* Pavona_slide	*Pavona gigantea* PGC3	*Pocillopora eydouxi* pocil_whole	*Pocillopora eydouxi* pocil_disep	*Porites sp* PNG fossil	*Porites sp* PNG modern	*Porites lobata* NA33_less_ dense	*Porites lobata* NA35_less_ dense	*Porites lobata* NA35_dense
E_f	−2.59 (28)	−3.51 (26)	−3.94 (24)	−2.59 (24)	−3.71 (25)	−4.36 (29)	−4.11 (35)	−3.30 (25)	−3.48 (26)	−15.24 (30)	−4.45 (29)	−4.33 (29)
σ^2_1	0.022 (1)	0.028 (1)	0.026 (1)	0.023 (1)	0.026 (1)	0.024 (1)	0.024 (2)	0.026 (1)	0.027 (1)	0.022 (1)	0.024 (1)	0.024 (1)
σ^2_2	0.037 (8)	0.029 (5)	0.036 (7)	0.037 (7)	0.035 (6)	0.032 (7)	0.033 (9)	0.035 (6)	0.035 (7)	0.038 (9)	0.032 (7)	0.035 (8)
σ^2_3	0.028 (3)	0.031 (3)	0.031 (3)	0.034 (3)	0.029 (3)	0.025 (3)	0.029 (4)	0.030 (3)	0.030 (3)	0.029 (4)	0.027 (3)	0.027 (3)
R_1	2.584 (4)	2.632 (3)	2.590 (3)	2.585 (3)	2.589 (3)	2.589 (4)	2.584 (5)	2.586 (3)	2.590 (4)	2.580 (4)	2.587 (4)	2.586 (4)
R_2	2.981 (19)	3.027 (12)	3.012 (15)	2.984 (16)	3.009 (15)	2.998 (17)	2.992 (22)	3.006 (15)	3.013 (15)	2.988 (21)	2.995 (18)	2.995 (19)
R_3	4.020 (11)	4.167 (10)	4.023 (10)	4.024 (10)	4.022 (10)	4.021 (11)	4.017 (14)	4.020 (10)	4.022 (10)	4.017 (12)	4.020 (11)	4.022 (11)
PERCA1	0.99 (F)	0.00 (F)	0.96 (11)	1.14 (14)	0.90 (11)	0.94 (7)	1.01 (17)	0.95 (8)	0.94 (7)	1.00 (15)	0.97 (9)	0.98 (9)
R (Fit)	24.0%	24.2%	22.7%	21.8%	23.5%	27.2%	30.5%	23.4%	24.6%	25.7%	27.0%	27.1%

Genus Sample name	*Porites lobata* Japan	*Porites lobata* Tarawa old	*Porites lobata* Tarawa modern	*Porites lutea* PB3	*Porites lutea* PB3_outer	*Porites lutea* PB3_untreat	*Porites lutea* PB4	*Porites lutea* PB4_outer	*Porites lutea* PB5_outer	*Porites lutea* PB6	*Porites lutea* PB6_outer
E_f	−2.66 (26)	−2.66 (25)	−2.87 (22)	−4.26 (24)	−12.78 (31)	−3.16 (33)	−3.13 (24)	−3.07 (23)	−11.43 (34)	−18.50 (32)	−4.44 (28)
σ^2_1	0.025 (1)	0.026 (1)	0.025 (1)	0.027 (1)	0.023 (1)	0.023 (2)	0.026 (1)	0.027 (1)	0.026 (2)	0.023 (2)	0.023 (1)
σ^2_2	0.033 (6)	0.034 (6)	0.033 (5)	0.037 (7)	0.031 (8)	0.031 (7)	0.036 (6)	0.041 (7)	0.030 (8)	0.040 (12)	0.035 (8)
σ^2_3	0.032 (3)	0.030 (3)	0.027 (3)	0.030 (3)	0.030 (4)	0.029 (4)	0.030 (3)	0.032 (3)	0.030 (4)	0.026 (4)	0.029 (4)
R_1	2.591 (4)	2.589 (3)	2.590 (3)	2.588 (4)	2.587 (4)	2.582 (4)	2.587 (3)	2.582 (3)	2.590 (5)	2.585 (5)	2.583 (4)
R_2	3.006 (14)	3.004 (14)	3.007 (13)	3.014 (15)	3.001 (18)	2.983 (18)	3.009 (14)	3.017 (15)	3.020 (18)	2.995 (25)	2.985 (19)
R_3	4.025 (10)	4.024 (10)	4.024 (9)	4.021 (11)	4.021 (13)	4.016 (13)	4.025 (10)	4.029 (10)	4.018 (14)	4.021 (12)	4.023 (12)
PERCA1	0.99 (12)	0.97 (12)	0.91 (5)	0.87 (11)	1.00 (12)	0.97 (12)	0.96 (8)	0.94 (7)	0.97 (11)	1.00 (10)	1.01 (11)
R (Fit)	22.2%	23.4%	20.6%	24.2%	27.3%	28.9%	22.0%	21.4%	29.3%	28.1%	26.3%

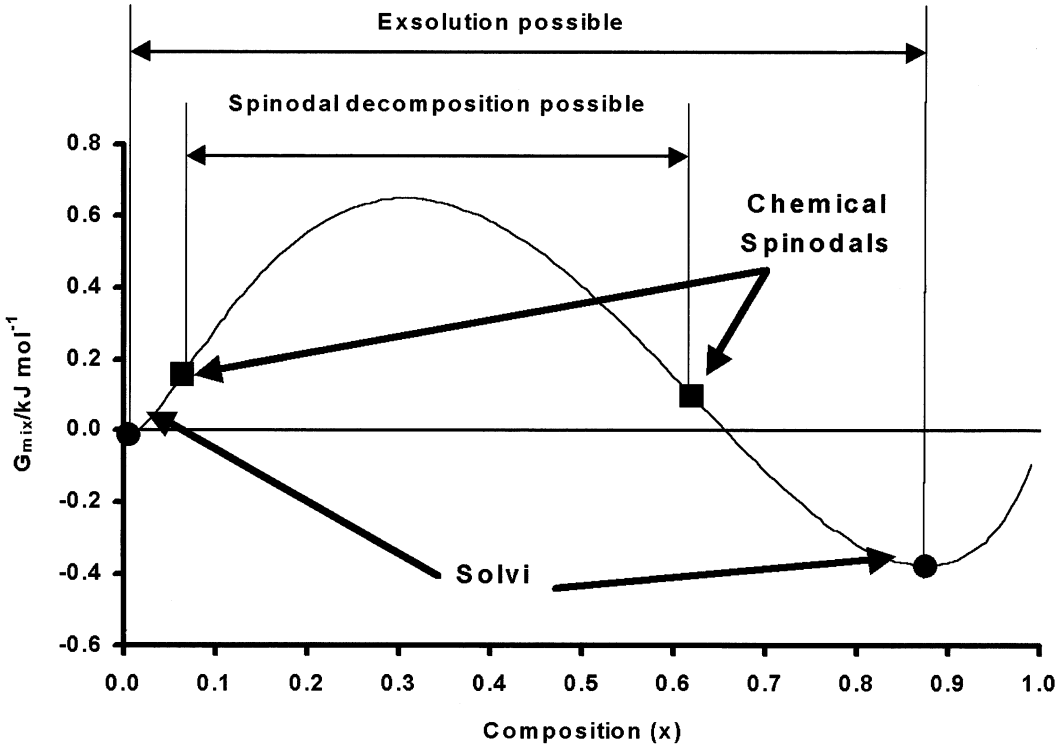

Fig. 2. Free energy profile of the aragonite-strontianite system based on the data of Plummer and Busenberg (1987). The two minima in the profile correspond to the Ca-rich and Sr-rich parts of the solvus and points of inflexion are the chemical spinodals. The region for $0.0<x<0.1$ (containing the Ca-rich part of the solvus) is enlarged in Fig. 3.

refinements, which should increase to >4.020 Å as PERCA1 falls, refine to values indistinguishable from that of the aragonite standard (see above). Therefore none of the refinements indicate partly ordered states that might have arisen from spinodal decomposition.

Exsolution by spinodal decomposition can only be initiated if the sum of the free energies of mixing of all transition states during exsolution are less than or equal to the free energy of mixing of the initial material (see Putnis, 1992 for a review of this and other thermodynamic principles). Materials require a significant compositional contrast between the composition of the phase and the locus of the solvus to fulfil this condition, and the position at which this condition is first achieved is called the chemical spinodal (Fig. 2). As a result, there is a compositional window between the solvus and chemical spinodal, where exsolution, although favoured, does not have a sufficiently large free energy contrast to start. Figure 2 is an estimate of the free energy profile of the aragonite-strontianite solid solution using values of enthalpy and entropy from Plummer and Busenberg (1987). These authors modelled the free energy of mixing profile of the system as:

$$G = RT[x \ln x + (1 - x)\ln(1 - x)] + x(1 - x)[A_0 + A_1(2x - 1)]$$

where: $\boldsymbol{G}$ is the free energy of mixing of a particular phase in the solid solution in kJ mol^{-1},

$\boldsymbol{R}$ is the molar gas constant (8.315 J K^{-1}mol^{-1})

$\boldsymbol{x}$ is the composition in the solid solution $sr_xCa_{(1-x)}CO_3$

and $\boldsymbol{A}_0$ and $\boldsymbol{A}_1$ are constants with values 8.49±0.30 and −4.51±0.20 kJ mol^{-1} (Plummer and Busenberg, 1987).

The solubility limits (solvus) of Sr in aragonite and Ca in strontianite are given by solutions to the equation $^{dG}/_{dx}=0$, and were estimated at x=0.0058 (5.8 mmol mol^{-1}, ~5100 ppm Sr) and x=0.875 (~520 000 ppm Sr). The loci of the chemical spinodal are given by the solutions of the second order differential $^{d2G}/_{dx2}=0$ and were estimated at x=0.065 (~57 000 ppm Sr) and x=0.62 (~368 000 ppm Sr) (Plummer and Busenberg, 1987). The composition of coral aragonite lies at x~0.0085 (~7500 ppm, 8.5 mmol mol^{-1}), i.e., in the compositional window between the solvus and the chemical spinodal (Fig. 3). Coral aragonite is therefore in principle thermodynamically unstable, but is not sufficiently Sr-rich for spinodal decomposition to start.

The third possible mechanism for exsolution in this system, applicable to all compositions within the solvus, is the direct nucleation of strontianite domains. We can estimate the rate of such exsolution from the diffusion rate of Sr in aragonite. Unfortunately, we know of no measurements of this value in the open literature, but data for Sr diffusion in for other materials such as calcite (Cherniak, 1997) are published. Calcite and aragonite are ionic solids with the same composition and therefore their diffusivities are likely to be similar to within a few orders of magnitude. The diffusivity of Sr in calcite at 25°C is estimated as ~10^{-36} m^2 s^{-1} using Cherniak's (1997) data. Assuming similar diffusivities in aragonite, we estimate that timeperiods of ~10^{17} yr are required for the nucleation of

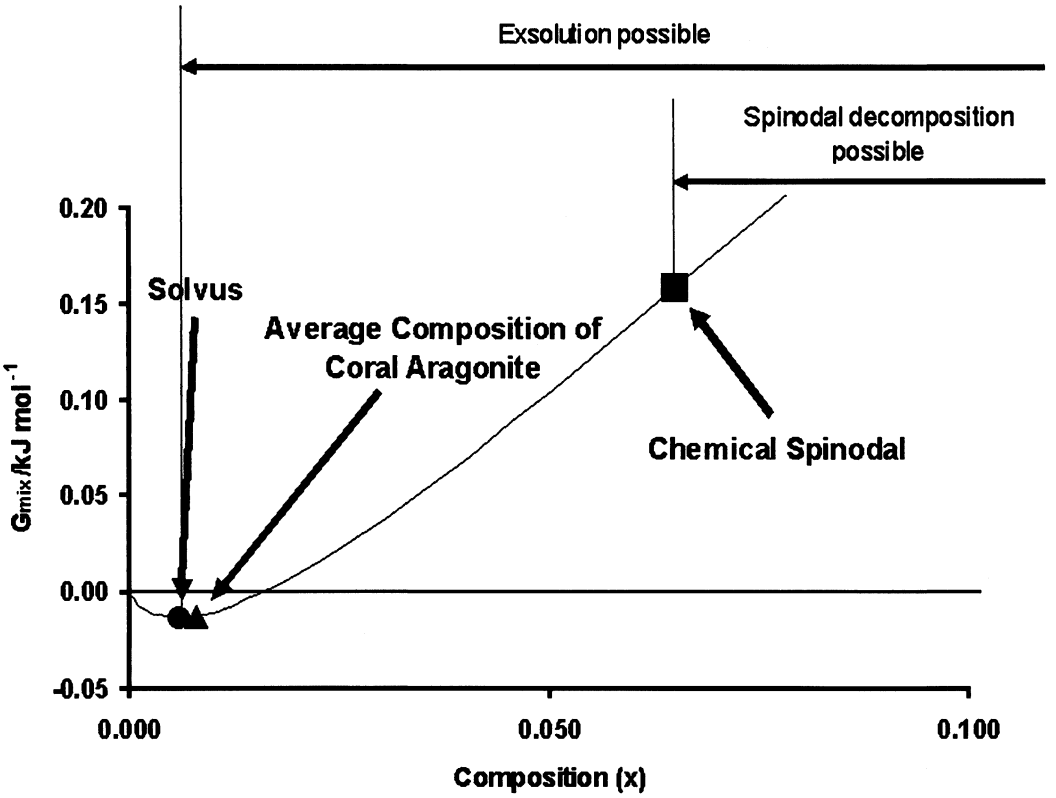

Fig. 3. Enlargement of Fig. 2 for the region $0.0<x<0.1$ showing the average composition of coral aragonite and the position of the solvus in the Sr-poor half of the system. Note that the composition of coral aragonite is more Sr-rich than the solvus.

nm-size strontianite domains in aragonite. Such analysis is clearly only a rough estimate with several limitations (e.g., it extrapolates far beyond the temperature range of Cherniak's experimental data), but it indicates that direct nucleation of strontianite is unlikely even over geological timescales.

Our EXAFS measurements include coral aragonite of a variety of ages, including material from Huon peninsula in Papua New Guinea that is ~130 kyr old (Tudhope et al., 2001). None of the samples show evidence for calcite from XRD or in thin section, hence significant breakdown by solution reprecipitation has not occurred. Furthermore refinement of R_3 and PERCA1 (indicative of the state of Sr order) in the fossil sample is indistinguishable from the refinements of the recent corals and the Sr in aragonite standard. None of the fits are improved by modelling as a two-phase mixture, showing that significant amounts (>5% of the Sr) of primary strontianite-rich domains have not been formed in the aragonite. These data suggest there is no exsolution by any mechanism in the Sr-supersaturated aragonite up to ~130 kyr.

Coral aragonite is a metastable phase, but our analysis of the kinetics of the system suggests that exsolution by solid state diffusion is unlikely even over protracted geological timescales. Our study has included some of the oldest material used for environmental reconstructions (the Huon peninsula corals of Tudhope et al., 2001, at $\sim 10^5$ yr), but there is expanding interest in studying the geochemistry of older fossil corals. Our data show that coral seawater archives in the aragonite studied are metastable, so long as solution reprecipitation has not occurred. Such replacement would be recognized by changes in texture in thin section and by calcite in XRD analyses. Furthermore, our analysis of the diffusion kinetics suggests such metastability extends indefinitely into the geological past.

Although we demonstrate no variation in the bulk structural state of all the corals studied, it remains possible that structural contrasts exist between particular parts of the coral skeletal architecture. Many individual components of the coral skeleton (e.g., centres of calcification and dissepiments) comprise <5% of the total aragonite volume, and therefore different structural states in these components would not be resolved in refinements of the bulk. Although a detailed analysis of the relationships between microstructure and Sr coordination is beyond the present study, we have here analyzed the dissepiments of a *Pocillopora eydouxi* sample and contrasted the results with the bulk response of the same coral. We observed that the structural state of the dissepiments was indistinguishable from the bulk, and conformed to ideally substituted Sr in aragonite. A more detailed analysis of the relationships between Sr structural state and skeletal architecture using micro-EXAFS is underway.

6. CONCLUSION

Our Sr K-EXAFS analyses indicate that corals precipitate a Sr-supersaturated aragonite and strontianite is not detectable in any of the samples. Sr coordination does not vary between taxa,

individuals and the age of the material analyzed. Variation in Sr structural state is therefore not responsible for the different ways in which each of these corals encodes the local SST. Treating the samples in sodium chlorate(I) also has no effect on the coral Sr K-edge EXAFS. Furthermore, our analysis of the thermodynamics and kinetics of the aragonite-strontianite solid solution suggests that coral aragonite is a metastable phase with such slow diffusion kinetics that diffusion-related decomposition will not occur within geological timeframes. Although compositional modification may still occur by solution/reprecipitation, this is recognizable as textural change in thin section, and by XRD as the formation of calcite. Therefore coral aragonite of all ages is potentially useful in the reconstruction of past environments in all of the taxa studied.

Acknowledgments—Bob Bilsborrow of Daresbury Laboratories is thanked for his help on the 16.5 station. Jeremy Dobson provided support on the Daresbury beamlines. Fred Mosselmans provided invaluable support in the use of EXCURV98 and Ian Harvey helped with EXSPLINE. The present study was supported by a NERC Standard grant. Nick Pingitore, Sandy Tudhope, Stewart Fallon, Julia Cole and Glen Shen are thanked for providing coral samples for the present study. The manuscript benefited from the reviews of Andrea Cicero and two anonymous referees.

Associate editor: T. Lowenstein

REFERENCES

Alibert C. and McCulloch M. T. (1997) Strontium/calcium ratios in modern Porites corals from the Great Barrier Reef as a proxy for sea surface temperature: Calibration of the thermometer and monitoring of ENSO. *Paleoceanography* **12,** 345–363.

Allison N., Tudhope A. W., and Fallick A. E. (1996) A study of the factors influencing the stable carbon and oxygen isotopic composition of *Porites lutea* coral skeletons from Phuket, South Thailand. *Coral Reefs* **15,** 43–57.

Allison N., Finch A. A., Sutton S. R., and Newville M. (2001) Strontium heterogeneity and speciation in coral aragonite: Implications for the strontium palaeothermometer. *Geochim. Cosmochim. Acta* **65,** 2669–2767.

Allison N., Finch A. A. (2002) Sr/Ca in Coral Aragonite: Is Night Carbonate a Good Indicator of Sea Surface Temperatures? *EOS Trans. AGU*, **83**(47)**,** Fall Meet. Suppl., Abstract PP52B-04.

Barnes D. J. and Lough J. M. (1993) On the nature and causes of density banding in massive coral skeletons. *J. Exp. Mar. Biol. Ecol.* **167,** 91–108.

Beck J. W. (1994) Sea-surface temperature from coral skeletal strontium calcium ratios. *Science* **264,** 891.

Beck J. W., Edwards R., Ito E., Taylor F. W., Recy J., Rougerie F., Joannot P., and Henin C. (1992) Sea-surface temperature from coral skeletal strontium calcium ratios. *Science* **257,** 644–647.

Cherniak D. J. (1997) An experimental study of strontium and lead diffusion in calcite, and implications for carbonate diagenesis and metamorphism. *Geochim. Cosmochim. Acta* **61,** 4173–4179.

Cole J. E., Fairbanks R. G., and Shen G. T. (1993) Recent variability in the southern oscillation - isotopic results from a Tarawa atoll coral. *Science* **260,** 1790–1793.

de Villiers S., Nelson B. K., and Chivas A. R. (1995) Biological controls on coral Sr/Ca and $\delta^{18}O$ reconstructions of sea surface temperatures. *Science* **269,** 1247–1249.

de Villiers S., Shen G. T., and Nelson B. K. (1994) The Sr/Ca-temperature relationship in coralline aragonite: Influence of variability in (Sr/Ca)seawater and skeletal growth parameters. *Geochim. Cosmochim. Acta* **58,** 197–208.

Fallon S. J., McCulloch M. T., van Woesik R., and Sinclair D. J. (1999) Corals at their latitudinal limits: Laser ablation trace element systematics in Porites from Shirigai Bay, Japan. *Earth Plant Sci. Lett.* **172,** 221–238.

Finch A. A., Allison N., Sutton S. R., Newville M. (2003) Strontium in coral aragonite: 1. Characterisation of Sr coordination by EXAFS. *Geochim. Cosmochim. Acta* **67,** 1189–1194.

Greegor R. B. Pingitore N. E., Jr., and Lytle F. W. (1997) Strontianite in coral skeletal aragonite. *Science* **275,** 1452–1454.

Marshall J. F. and McCulloch M. T. (2002) An assessment of the Sr/Ca ratio in shallow water hermatypic corals as a proxy for sea surface temperature. *Geochim. Cosmochim. Acta* **66,** 3263–3280.

McCulloch M. T., Tudhope A. W., Esat T. M., Mortimer G. E., Chappell J., Pillans B., Chivas A. R., and Omura A. (1999) Coral record of equatorial sea-surface temperatures during the penultimate deglaciation at Huon Peninsula. *Science* **283,** 202–204.

Plummer L. N. and Busenberg E. (1987) Thermodynamics of aragonite-strontianite solid solutions: Results from stoichiometric solubility at 25 and 76°C. *Geochim. Cosmochim. Acta* **51,** 1393–1411.

Putnis A. (1992) *Introduction to Mineral Sciences*. Cambridge University Press, Cambridge, UK.

Rimstidt J. D., Balog A., and Webb J. (1998) Distribution of trace elements between carbonate minerals and aqueous solutions. *Geochim. Cosmochim. Acta* **62,** 1851–1863.

Shen G. T., Linn L. J., Campbell T. M., Cole J. E., and Fairbanks R. G. (1992) A chemical indicator of trade-wind reversal in corals from the western tropical pacific. *J. Geophys Res-Oceans* **97,** 12689–12697.

Tudhope A. W., Chilcott C. P., McCulloch M. T., Cook E. R., Chappell J., Ellam R. M., Lea D. W., Lough J. M., and Shimmield G. B. (2001) Variability on the El Nino-Southern Oscillation through a glacial Interglacial Cycle. *Science* **291,** 1511–1517.